INVESTIGATION OF DYNAMIC MOORING MODEL AND MOTION RESPONSES OF MOORED FLOATING BODY USING MPS-DEM COUPLING METHOD

Yijie Sun [1], Guang Xi [1] Zhongguo Sun [1]

[1] School of Energy and Power Engineering, Xi'an Jiaotong University
Xi'an 710049, China
sun.zg@mail.xjtu.edu.cn

Keywords MPS, DEM, FSI, moored floating body

Abstract The interaction between the free surface and the moored floating body with restriction of the mooring line is a typical strongly nonlinear FSI problem. The wave provides the driving force and the mooring line gives the restrictive condition. In order to simplify the interactions between the wave, the floating body and the mooring line, the hypothesis was usually proposed as the mooring line was very thin and the mass could be neglected. Based on this theory, the interaction between the mooring line and the wave is ignored no matter the mooring line is slack or tensioned during calculation. However, in reality, the mooring line is usually made to be heavy to decrease the influence of wave impact and to limit the motion of floating structure.

In this paper, the hypothesis is canceled, and the interactions among the wave, the mooring line and the floating body are all considered. To solve this complex problem, a fully Lagrangian coupled method has been developed to analyze the motion response of the moored floating body under wave impact. The Moving Particle Semi-implicit (MPS) method has been applied to model the fluid domain, while the Discrete Element Method (DEM) with a parallel bond model is used to represent the floating body and the mooring line. A new mooring line model was proposed based on the DEM. Compared with other model, the proposed model not only takes the mooring line stretching, bending and torsion into consideration, but also avoids mesh construction and has less mathematical operations.

A bending cantilever beam case is carried out to validate the DEM model for deformable mass. The results show that the present DEM method can calculate the forces and the deformation of the flexible structure correctly. Furthermore, the motion responses of a moored floating body under wave impact are calculated using the coupled method. The motions and deformation of the floating body and the mooring line are shown in time series.

1 INTRODUCTION

The exploitation and utilization of the ocean resources rely on all kinds of offshore facilities such as oil rigs, wind turbine platforms, and wave energy converters etc [1]. To keep the stability in deep water, these floating facilities are often anchored by mooring lines to the seabed. The motion of a floating platform would be affected by not only the wave impact, but also the force given by mooring lines. Thus, the mooring system is an important component element to the offshore facility and should be considered into the motion analysis of the offshore structure.

Catenary mooring lines and tensioned mooring lines are most commonly used mooring lines in the ocean engineering [2-4]. Catenary mooring lines are long, heavy chain lines or

wires hanging freely and connecting the platform and the seabed. Catenary mooring lines act horizontal forces on the floating platform to restrict the surge, sway and yaw degrees of freedom [1]. Tensioned mooring lines are usually short, light, elastic lines, and are stretched to connect the platform and the seabed by an inclined angle. The elastic forces due to the tautness would restrict the platform in six degrees of freedom.

The deformation and the motion of the mooring lines could be influenced by the nonlinear hydrodynamic drag forces from the wave and the friction forces from the seabed. Once influenced, the forces the mooring lines exerting on the floating structure are changed and the motion of the structure would be restricted. The mooring system have a great effect on the motion of the floating structure, especially in the large amplitude wave conditions. Thus, to improve the accuracy in the motion analysis of the floating structure, a number of the numerical models have been developed to simulate the mooring system [5].

Force displacement velocity model, is a simple model and easy to implement [6]. In this model, the mooring force is nonlinear or linear to the displacement and velocity. This model could not calculate the mooring forces and is not accuracy in the motion analysis of the floating structure. To improve this model, the quasi-static model is proposed [7-10]. The quasi-static model takes the buoyancy forces, elastic stretching and seabed friction into consideration, and it could be applied to simulate both catenary and tensioned mooring lines. However, this model ignores the hydrodynamic forces the wave gives on the mooring lines, as well as the damping of the mooring lines. Both force displacement velocity model and the quasi-static model are based on the force equilibrium assumption, where the inertial of the mooring line would be neglected.

To overcome the shortcomings of the force equilibrium assumption, some dynamic models are developed as the multibody model and finite element model. The lumped mass method (LMM) is often used in the multibody model [11]. The mooring line is divided into several rigid or elastic elements which have an elastic-damping relationship with each other. Though the multibody model considers the hydrodynamic forces and the inertial of the mooring line, the damping and stiffness of the mooring line are not taken into account. Another dynamic model, finite element model [12-14], takes all the influence factors into consideration, including the damping and stiffness of the mooring line. However, in this model, mesh generation and the complex mathematical formulation of the mooring line would bring more costs in computational efficiency.

In this paper, the DEM model was applied to simulate the mooring system. The mooring line is composed of a number of particles, and particles bond with each other by the particle-particle model and parallel bond model in DEM. In this way, the inertial, damping and stiffness of the mooring line would be considered in the calculation. Moreover, a two-way solid-fluid coupling model was established using MPS-DEM method, and the hydrodynamic forces the wave exerting on the mooring line could be calculated. A mooring line model based on the Lagrangian method was proposed, and a full Lagrangian-Lagrangian method was developed for the motion analysis of the moored floating structure.

2 NUMEICAL METHODS

The MPS method is used to calculate for the fluid phase while DEM is for the solid phase, and a two-way fluid-solid coupling model is applied to simulate the interaction between fluid and solid. The algorithms of the MPS method and the DEM are briefly introduced here, more details and systematical descriptions could be found in other articles [15-17].

2.1 MPS METHOD

The MPS method was first proposed by Koshizuka [18], and was applied to simulate the incompressible fluid. The governing equations are given in the Lagrangian form as:

$$\frac{D\rho}{Dt}+\rho\frac{\partial u_i}{\partial x_i}=0 \tag{1}$$

$$\rho\frac{Du_i}{Dt}=-\frac{\partial p}{\partial x_i}+\frac{\partial \tau_{ij}}{\partial x_j}+\rho f_i \tag{2}$$

The kernel function is defined as:

$$W(r)=\begin{cases}\dfrac{r}{r_e}-1 & (r<r_e)\\ 0 & (r<r_e)\end{cases} \tag{3}$$

Where r is the distance between two particles; r_e is the interaction radius of particles.

The Laplacian operator is formulated as:

$$\left\langle\nabla^2\varphi\right\rangle_i=\frac{2d}{\lambda n^0}\sum_{j\neq i}\left(\varphi_j-\varphi_i\right)w\left(\left|\boldsymbol{r}_j-\boldsymbol{r}_i\right|\right) \tag{4}$$

The gradient operator applied in this paper was improved by Zhang [19] to overcome the drawback in original gradient operator and conserve the linear and angular momentum of the system:

$$\left\langle\nabla\varphi\right\rangle_i=\frac{d}{n^0}\sum_{j\neq i}\frac{\varphi_j+\varphi_i}{\left|\boldsymbol{r}_j-\boldsymbol{r}_i\right|^2}\left(\boldsymbol{r}_j-\boldsymbol{r}_i\right)w\left(\left|\boldsymbol{r}_j-\boldsymbol{r}_i\right|\right) \tag{5}$$

The Pressure Poisson equation (PPE) in this paper is defined as:

$$\left\langle\nabla^2 p^{k+1}\right\rangle_i=(1-\gamma)\frac{\rho}{\Delta t}\nabla\cdot u_i-\gamma\frac{\rho}{\Delta t^2}\frac{<n^k>_i-n^0}{n^0} \tag{6}$$

Where γ is a blending parameter which varies from 0 to 1. In this study, γ is 0.008 in order to reduce the error of pressure.

2.2 DEM

In DEM, two particles would be defined as a contact when the distance of their mass center is smaller than the sum of their radius. The contact force could be calculated by the contact model. The motion of particles obeys Newton's Second Law.

The governing equations of solid phase are:

$$m\frac{\mathrm{D}\boldsymbol{u}}{\mathrm{D}t}=\sum\boldsymbol{F}_c+\boldsymbol{F}_{ls}+\boldsymbol{F}_g \tag{7}$$

Where m and $\boldsymbol{u}$ are mass and velocity of each particle respectively. $\boldsymbol{F}$ is the force. The subscript *c* represents contact between two particles; the subscript *ls* means the interaction

between fluid and solid, while the subscript *g* stands for the gravitational force.

The contact between particles contains a spring and a dashpot, as well as a friction slide, as shown in Fig. 1. The contact force can be decomposed in tangential and normal direction, and could be calculated by Eq. (8). The contact force in each direction contains a spring force and a damping force, seen in Eq. (9). When the tangential force is larger than the maximum static friction force, it will equal to the sliding friction force.

$$\boldsymbol{F}_c = \boldsymbol{F}_{cn} + \boldsymbol{F}_{ct} \tag{8}$$

Where the subscript *n* represents the normal direction, and the subscript *t* represents the tangential direction.

$$F_{cn} = -k_n \delta_n - d_n u_n \tag{9}$$

$$F_{ct} = \begin{cases} -k_t \delta_t - d_t u_t & (|F_{ct}| < f\,|F_{cn}|) \\ -|F_{cn}| \cdot u_t / |u_t| & (|F_{ct}| \geq f\,|F_{cn}|) \end{cases} \tag{10}$$

Where k, d, f, δ and u are stiffness, damping coefficient, friction coefficient, displacement and velocity of each particle.

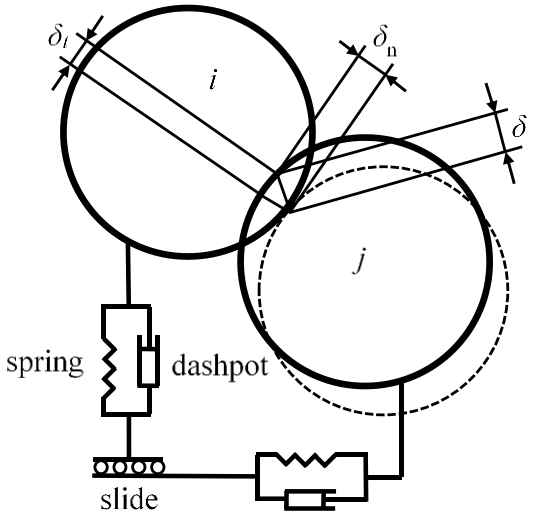

Figure 1 Contact model in DEM

To model the structural behavior, the bonded-particle model (BPM) was introduced to the DEM. The BPM was first developed by Potyondy and Cundall [15] to model rock behaviors, and it uses discrete particle bonding relationship to describe constitutive solid behaviors. In BPM, the motions of bond particles are determined by two kinds of contact models, the particle-particle contact model and the parallel bond contact model. In different contact models, the stiffness, damping coefficient, and the contact area between two particles are defined differently, as shown in Fig. 2 [20].

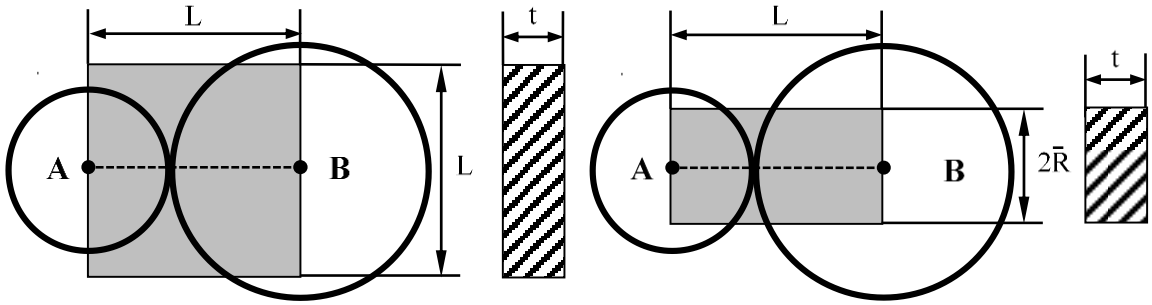

(a) (b)

Figure 2 Bond particle model: (a) particle-particle contact (b) parallel bond contact

According to the beam theory, the equivalent normal stiffness of two particles is related to the Young's modulus of the material.

$$k_n = \frac{AE}{L} = \frac{tLE}{L} = Et \tag{11}$$

Where E is the Young's modulus; A is the contact area. The contact volume of bonded particles should be $L \times L \times t$ m^3 in the particle-particle contact model, while in the parallel bond contact model it is $L \times 2\bar{R} \times t$ m^3. The damping normal coefficients could be derived from the following equation:

$$d_n = 2\beta\sqrt{mk_n} \tag{12}$$

Where β is the tuning parameter, which equals to 0.2 in this paper. When the maximum tensile stress exceeds the tensile strength, the parallel bond breaks and all the forces in parallel bond contact would be zero. However, the particle-particle contact model would be still in effect unless two particles are not in contact.

$$\bar{\sigma}_{\max} = \frac{-\bar{F}_n}{A} + \frac{|\bar{M}|\bar{R}}{I} \tag{13}$$

Where $\bar{\sigma}_{\max}$ is the maximum tensile stress, M is the resultant moment.

3 NUMERICAL SIMULATION

3.1 CANTILEVER BEAM

To verify the reliability of the DEM, an oscillating cantilever beam is calculated. The geometry of the test case is shown in Fig. 3. The beam has a length of 0.2 m and a width of 0.02 m, and an initial velocity distribution was subjected on the beam [21], shown in Eq. (14). The bulk and shear modulus of the beam is 3.25×10^6 N/m^2 and 7.15×10^6 N/m^2.

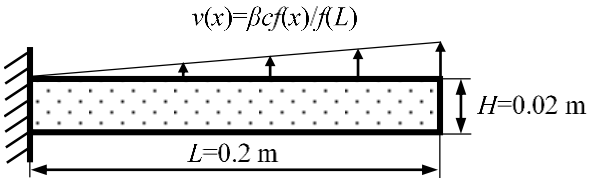

Figure 3 The description of the cantilever beam

$$v(x) = \beta c \frac{f(x)}{f(L)}$$

$$f(x) = (\cos k_w L + \cosh k_w L)(\cosh k_w x - \cos k_w x) + (\sin k_w L - \sinh k_w L)(\sinh k_w x - \sin k_w x) \quad (14)$$

Where v represents the vertical velocity of the particle; β is the velocity amplification factor, which equals to 0.01 in this paper; c stands for the speed of the sound; k_w is the wave number and could be obtained by Eq. (15).

$$\cos(k_w L)\cosh(k_w L) = -1 \quad (15)$$

The cantilever beam would oscillate due to the velocity field prescribed at the initial moment. The deflection at the free end of the beam is calculated and the result shows a good agreement with the analytical solution. It could be seen in the figure 5 that the stress field of the beam is stable and smooth.

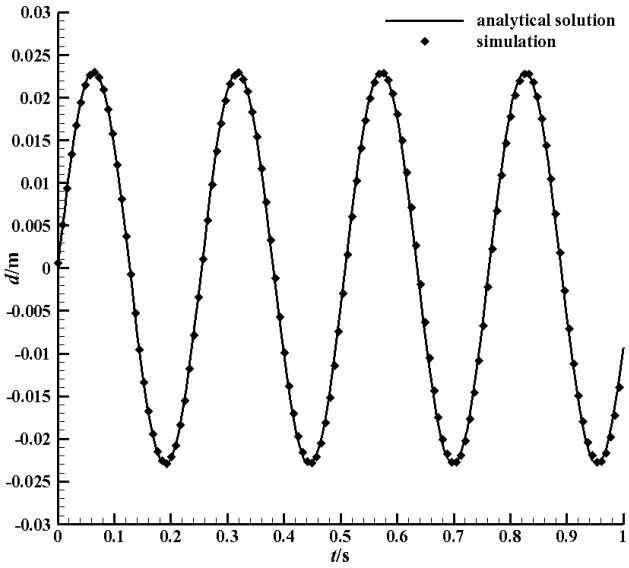

Figure 4 The deflection at the free end of the cantilever beam

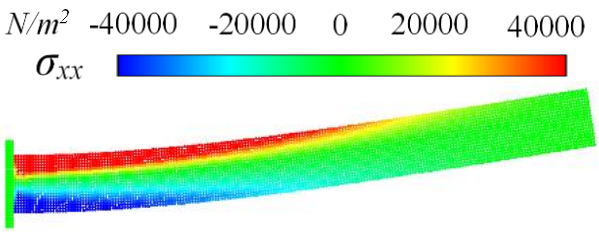

Figure 5 The stress field at t =0.57 s

3.2 MOORED FLOATING STRUCTURE

In this section, the motion of a rectangle floating structure with four mooring lines under regular wave was simulated. The motion response and the stress field of the floating structure was studied and the mooring force distribution was shown.

3.2.1 MOORING SYSTEM MODEL

Several mooring system models have been developed, as force displacement velocity model, the quasi-static model, the multibody model and finite element model. Table 1 compares the features of these models.

Table 1 Comparison of different mooring system models.

	Force displacement velocity	Quasi-static	Multibody	Finite element	present
Static force	√	√	√	√	√
Line-seabed interaction		√	√	√	√
Elastic stretching		√	√	√	√
Bending stiffness			√	√	√
Torsional stiffness				√	√
Inertia, damping, hydrodynamic			√	√	√

The mooring system model used in this paper is based on the DEM. The mooring line is composed of a number of particles. Given the Young's modulus and the shear modulus of the mooring line, the stiffness and damping coefficient in normal and tangential directions between the neighbouring particles would be determined. The motion behaviour of the mooring line contains stretching, bending and torsion. Moreover, the inertia of the line, the friction on the seabed and the hydrodynamic force the wave giving to the line are taken into consideration as well.

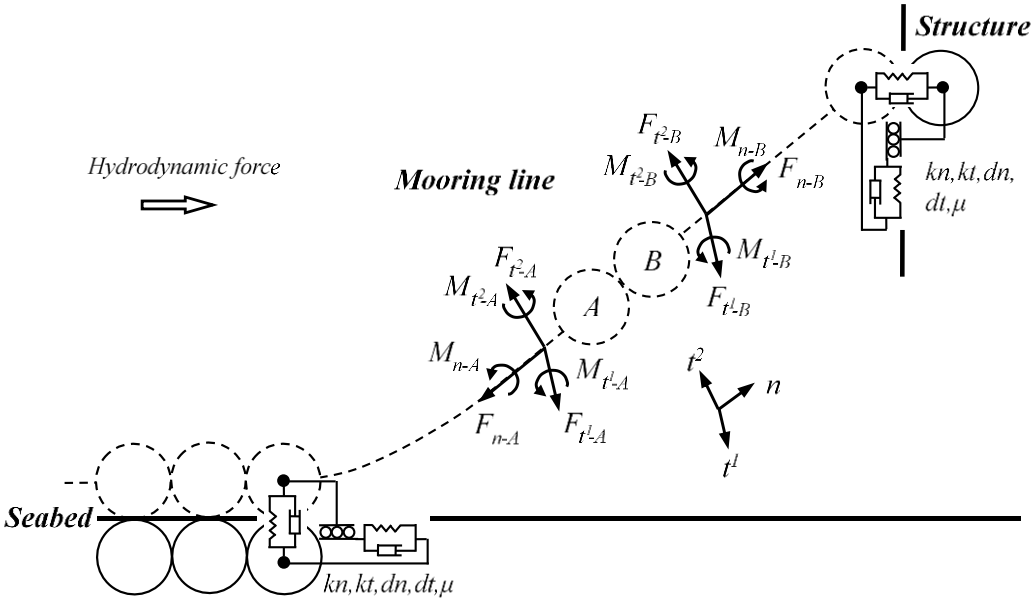

Figure 6 Mooring system presentation

One obvious benefit of the mooring system model in this paper is that all the factors listed in the table 1 are considered. What's more, the model could be implemented more easily than the finite element model, as its mathematical formulation is less complex and there is no need for mesh generation.

3.2.2 MOTION OF MOORED FLOATING STRUCTURE

The motion response of a floating structure with four tensioned mooring lines under regular wave was studied. In three dimensions, a floating structure has six degree of freedom, which are surge, sway, heave, yaw, pitch, roll respectively. More detailed are shown in figure 7. These six motion responses could be used to quantitively describe the motion and evaluate the stability of the floating structure.

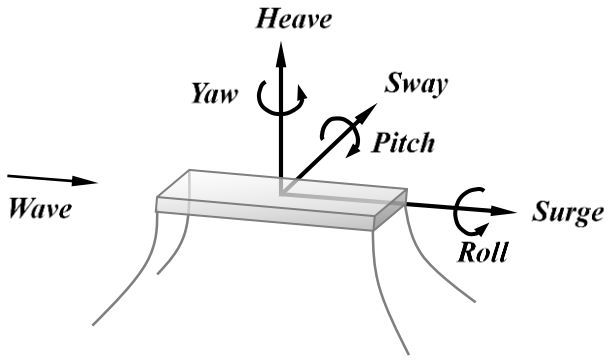

Figure 7 Description of motion responses of floating structure.

Figure 8 illustrates the initial geometry model of the calculation. The left boundary of the wave tank is a piston-type wave maker to generate regular wave. The floating structure is moored at the bottom by four tensioned mooring lines. The damping area is to make sure there is no reflected wave back to the floating structure.

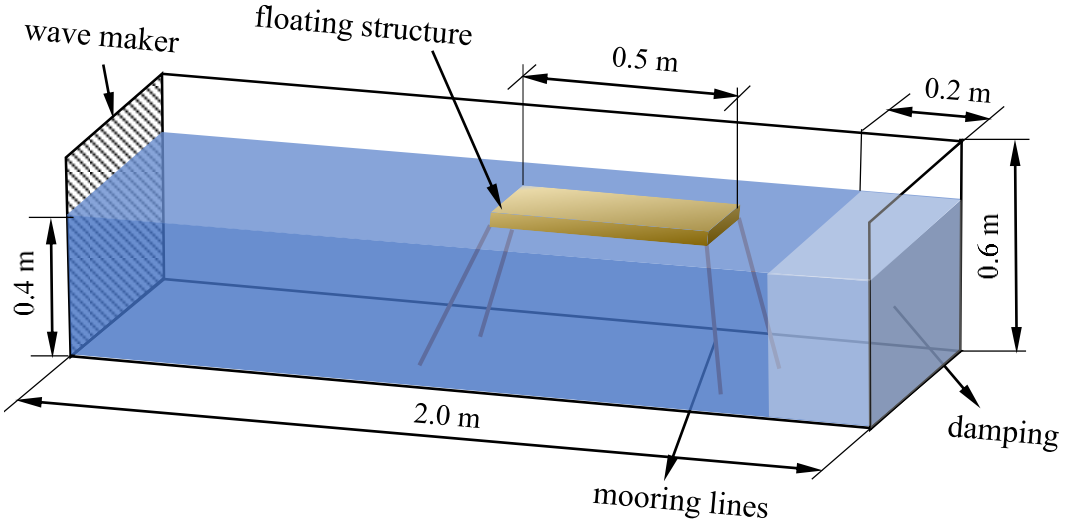

Figure 8 Schematic of the computational domain.

The mooring lines are set to be straight at the initial time and in the influence of the floating structure and the wave, the mooring lines would bend and deform, seen in figure 9. Figure 9 shows the motion of the floating structure in one time period of regular wave. The right column shows the shape of the mooring line at the same time. Under the wave impact, the structure

moves downstream while the two front mooring lines become stretched (*t*=3.2s~3.4s). The mooring lines would generate forces to limit the motion of the floating structure. The structure stops moving with the wave and begin to sink. The wave casts up on the structure. As the wave passes by, the structure would go back to the initial position under the mooring force and the front mooring lines become slack (*t*=3.6s~3.8s).

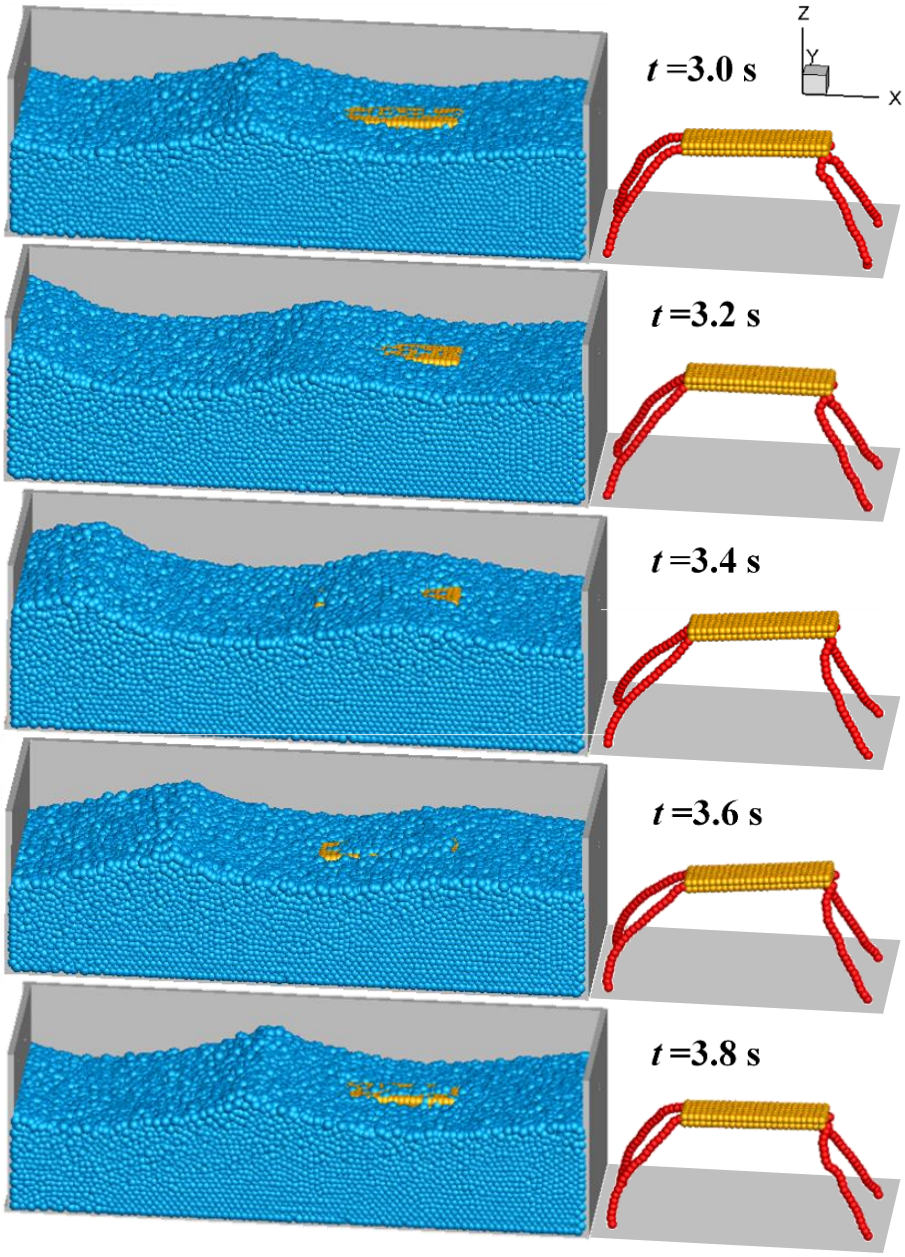

Figure 9 Motion of the floating structure in different time.

Figure 10 shows the relative surge, heave and sway response of the floating structure. At the initial time, the structure sinks under gravity, and becomes stable with a draught of around 0.04 m. At about t=2.0s, the first wave reaches the structure, and then the surge and heave responses begin to change regularly with a time period of 0.8 s, which is equal to the time period of the wave. The sway response is more stable, mainly because its direction is vertical to the wave propagation direction. Also, the mooring way would have an effect on the sway response.

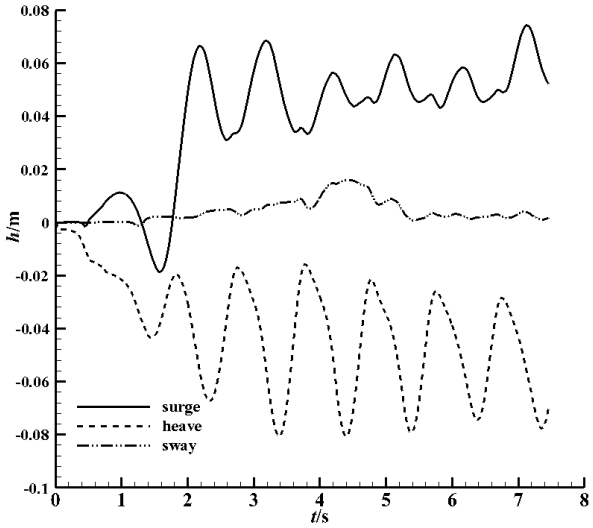

Figure 10 The surge, heave and sway response of the floating structure.

Similarly, the yaw and roll responses are in the plane that is vertical to the wave propagation plane, thus both values are small compared with the pitch response. The floating structure would rotate clockwise in the x-z plane during wave impact, shown in the figure 11. When the structure goes to the right extreme position (surge response is in the peak), the mooring line generates the largest mooring force. The structure sinks (heave response is in the valley) and begin to rotate anticlockwise (pitch response decreases).

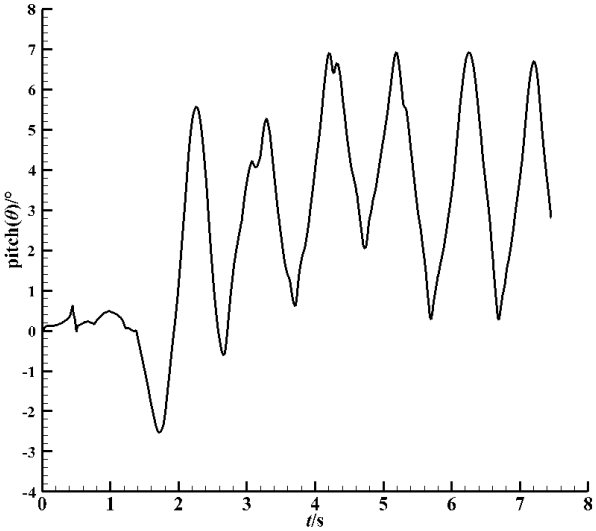

Figure 11 The pitch response of the floating structure.

4 CONCLUSION

In this paper, a new mooring line model was proposed based on the DEM. The proposed mooring line model takes the line damping, stretching and torsion into consideration, as well as the hydrodynamic and seabed forces, which makes it more accuracy in studying the motion of the mooring lines and the floating structure. Based on the Lagrangian framework, the new model avoids mesh construction and has less mathematical operations. Besides, it has strength showing the deformation of the mooring line at every time step and provide an important reference for the analysis of the mooring line-floating structure coupled system.

A full Lagrangian method was proposed to solve the non-linear fluid-solid interaction problem. The MPS method was used to simulate the wave motion while the DEM represents the solid phase, including the floating structure and the mooring line. A two-way solid-fluid coupling model was established. The wave makes a significant influence on the surge, heave and pitch responses. When the surge response becomes to the peak, the heave response becomes to the valley and the mooring lines are stretched to the limit and change the motion of the floating structure.

REFERENCES

[1] Rudman, M, & Cleary, P. W. (2016). The influence of mooring system in rogue wave impact on an offshore platform. *Ocean Engineering*, 115, 168-181.

[2] Borg, M., Shires, A., & Collu, M. (2014). Offshore floating vertical axis wind turbines, dynamics modelling state of the art. part I: aerodynamics. *Renewable and Sustainable Energy Reviews*, 39, 1214-1225.

[3] Kreuzer, E., & Wilke, U. (2003). Dynamics of mooring systems in ocean engineering. *Archive of Applied Mechanics*, 73(3-4), 270-281.

[4] Hall, M., Buckham, B., & Crawford, C. (2015). Evaluating the importance of mooring line model fidelity in floating offshore wind turbine simulations. *Wind Energy*, 17(12), 1835-1853.

[5] Chen, L., Basu, B., & Nielsen, Søren R.K. (2019). Nonlinear periodic response analysis of mooring cables using harmonic balance method. *Journal of Sound and Vibration*, 438, 402-418.

[6] Samadi, M., & Hassanabad, M. G. (2017). Hydrodynamic response simulation of Catenary mooring in the spar truss floating platform under Caspian Sea conditions. *Ocean Engineering*, 137, 241-246.

[7] Jonkman, J. M. (2009). Dynamics of offshore floating wind turbines-model development and verification. *Wind Energy*, 12(5), 459-492.

[8] Fan, T., Qiao, D., Yan, J., Chen, C., & Ou, J. (2017). An improved quasi-static model for mooring-induced damping estimation using in the truncation design of mooring system. *Ocean Engineering*, 136, 322-329.

[9] Barreiro, A, Crespo, A. J. C, Dominguez, J. M, Garcia-Feal, O, Zabala, I, & Gomez-Gesteira, M. (2016). Quasi-static mooring solver implemented in SPH. *Journal of Ocean Engineering and Marine Energy*, 2(3), 381-396.

[10] Fan, T., Ren, N., Cheng, Y., Chen, C., & Ou, J. (2018). Applicability analysis of truncated mooring system based on static and damping equivalence. *Ocean Engineering*, 147, 458-475.

[11] Zhu, X., & Yoo, W. S. (2016). Dynamic analysis of a floating spherical buoy fastened by mooring cables. *Ocean Engineering*, 121, 462-471.

[12] Gutiérrez-Romero, J. E., García-Espinosa, J., Serván-Camas, B., & Zamora-Parra, B. (2016). Non-linear dynamic analysis of the response of moored floating structures. *Marine Structures*, 49, 116-137.

[13] Kim, B. W., Sung, H. G., Kim, J. H., & Hong, S. Y. (2013). Comparison of linear

spring and nonlinear fem methods in dynamic coupled analysis of floating structure and mooring system. *Journal of Fluids and Structures*, 42, 205-227.

[14] Pham, H. D., Cartraud, P., Schoefs, F., Soulard, T., & Berhault, C. (2019). Dynamic modeling of nylon mooring lines for a floating wind turbine. *Applied Ocean Research*, 87, 1-8.

[15] Potyondy, D. O., & Cundall, P. A. (2004). A bonded-particle model for rock. *International journal of rock mechanics and mining sciences*, 41(8), 1329-1364.

[16] Cundall, P.A., Strack O.D.L. (1979). A discrete numerical model for granular assemblies. *Geotechnique* 29(1), 47-65.

[17] Koshizuka, S., & Oka, Y. (1996). Moving-particle semi-implicit method for fragmentation of incompressible fluid. *Nuclear science and engineering*, 123(3), 421-434.

[18] Koshizuka, S., Nobe, A., & Oka, Y. (1998). Numerical analysis of breaking waves using the moving particle semi‐implicit method. *International Journal for Numerical Methods in Fluids*, 26(7), 751-769.

[19] Zhang, S., Morita, K., Fukuda, K., & Shirakawa, N. (2006). An improved MPS method for numerical simulations of convective heat transfer problems. *International journal for numerical methods in fluids*, 51(1), 31-47.

[20] Zhang, X. P., & Wong, L. N. Y. (2012). Cracking processes in rock-like material containing a single flaw under uniaxial compression: a numerical study based on parallel bonded-particle model approach. *Rock Mechanics and Rock Engineering*, 45(5), 711-737.

[21] Khayyer, A., Gotoh, H., Falahaty, H., & Shimizu, Y. (2018). An enhanced ISPH-SPH coupled method for simulation of incompressible fluid-elastic structure interactions. *Computer Physics Communications*, S0010465518301759.